Accepted Manuscript

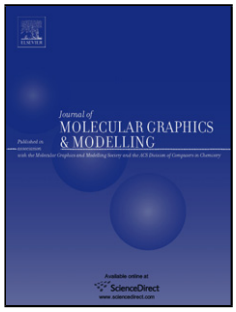

Title: Design and synthesis of a novel class of carbonic anhydrase-IX inhibitor 1-(3-(phenyl/4-fluorophenyl)-7-imino-3H-[1,2,3]triazolo[4,5d]pyrimidin 6 (7H)yl)urea

Author: Shikha Kumari Danish Idrees Chandra Bhushan Mishra Amresh Prakash Wahiduzzaman Faizan Ahmad Md. Imtaiyaz Hassan Manisha Tiwari

PII: S1093-3263(16)30006-7
DOI: http://dx.doi.org/doi:10.1016/j.jmgm.2016.01.006
Reference: JMG 6650

To appear in: *Journal of Molecular Graphics and Modelling*

Received date: 30-10-2015
Revised date: 11-1-2016
Accepted date: 16-1-2016

Please cite this article as: Shikha Kumari, Danish Idrees, Chandra Bhushan Mishra, Amresh Prakash, Wahiduzzaman, Faizan Ahmad, Md.Imtaiyaz Hassan, Manisha Tiwari, Design and synthesis of a novel class of carbonic anhydrase-IX inhibitor 1-(3-(phenyl/4-fluorophenyl)-7-imino-3H-[1,2,3]triazolo[4,5d]pyrimidin 6 (7H)yl)urea, Journal of Molecular Graphics and Modelling http://dx.doi.org/10.1016/j.jmgm.2016.01.006

Design and synthesis of a novel class of carbonic anhydrase-IX inhibitor 1-(3-(phenyl/4-fluorophenyl) -7-imino-3H-[1,2,3] triazolo[4,5d]pyrimidin 6 (7H)yl)urea

Shikha Kumari[a,†], Danish Idrees[b†], Chandra Bhushan Mishra[a†], Amresh Prakash[b†], Wahiduzzaman[b], Faizan Ahmad[b], Md. Imtaiyaz Hassan[b,*] and Manisha Tiwari[a,*]

[a]*Dr. B. R. Ambedkar Centre for Biomedical Research, University of Delhi, Delhi 110007, India*
[b]*Centre for Interdisciplinary Research in Basic Sciences, Jamia Millia Islamia, Jamia Nagar, New Delhi 110025, India*

[†]These authors equally contributed

*Corresponding Author

Md. Imtaiyaz Hassan, Ph.D.
(Assistant Professor)
Centre for Interdisciplinary Research in Basic Sciences,
Jamia Millia Islamia, Jamia Nagar, New Delhi 110025, India
E-mail: mihassan@jmi.ac.in

Dr. Manisha Tiwari
(Assistant Professor)
Dr. B. R. Ambedkar Centre for Biomedical Research,
University of Delhi, Delhi 110007, India
E-mail: mtiwari07@gmail.com

Graphical abstract

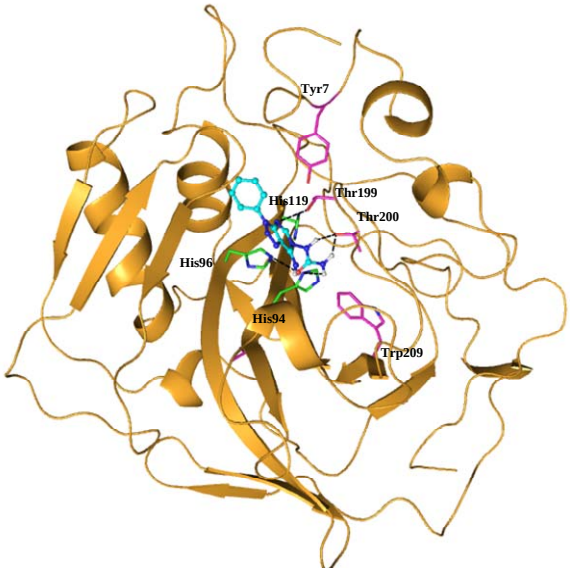

Cartoon view of TPUI docked with CAIX

Highlights

- Pyrimidine urea derived compound TPUI binds to CAIX with high affinity and selectivity.
- TPUI is preferentially docked in the active site cavity of CAIX.
- Fluorescence binding study is consistent with docking and MD simulation studies.
- TPUI appeared as novel class of CAIX inhibitor against hypoxia-induced cancer.

ABSTRACT

Carbonic anhydrase IX (CAIX) is a promising target in cancer therapy especially in the case of hypoxia-induced tumors. The selective inhibition of CA isozymes is a challenging task in drug design and discovery process. Here, we performed fluorescence-binding studies and inhibition assay combined with molecular docking and molecular dynamics (MD) simulation analyses to determine the binding affinity of two synthesized triazolo-pyrimidine urea derived (TPUI and TPUII) compounds with CAIX and CAII. Fluorescence binding results are showing that molecule TPUI has an excellent binding-affinity for CAIX (k_D= 0.048 μM). The TPUII also exhibits an appreciable binding affinity (k_D =7.52 μM) for CAIX. TPUI selectively inhibits CAIX as compared to TPUII in the 4-NPA assay. Docking studies show that TPUI is spatially well-fitted in the active site cavity of CAIX, and is involve in H-bond interactions with His94, His96, His119, Thr199 and Thr200. MD simulation studies revealed that TPUI efficiently binds to CAIX and essential active site residual interaction is consistent during the entire simulation of 40 ns. These studies suggest that TPUI appeared as novel class of CAIX inhibitor, and may be used as a lead molecule for the development of potent and selective CAIX inhibitor for the hypoxia-induced cancer therapy.

Keywords: Hypoxia-induced cancer; carbonic anhydrase IX inhibitor; drug design and discovery; triazolo-pyrimidine urea; MD simulation

1. Introduction

Carbonic anhydrase (CAs) are zinc containing metalloenzymes which primarily regulate physiological pH in human body [1]. CA catalyzes a rapid reversible conversion of carbon dioxide (CO_2) and water (H_2O) into a proton (H^+) and bicarbonate ion (HCO_3^-) which regulates the physiological processes connected with the transport of CO_2/ HCO_3^-, homeostasis, electrolyte secretion in a varieties of tissues/organs, biosynthetic reactions, respiration, calcification, tumorigenicity and bone reabsorption [2, 3]. In human there are 16 αCA isozymes have been reported which exhibit variable tissue distribution and functions [4].

CAIX is an attractive target for cancer treatment because of its limited expression in the normal tissues and predominant expression in varieties of tumour cells [5, 6]. CAIX is a hypoxia-inducible protein that regulates cellular pH to encourage cancer cell survival and invasion in the hypoxic microenvironments and serve as a potential biomarker in the poor prognosis of breast cancer metastasis and survival [7-9]. Furthermore, extracellular location of this isozyme is favourable for designing of a selective inhibitor which inhibits the membrane associated CAs without interacting to other cytosolic and mitochondrial CAs [10-12]. Expression of CAIX is induced under hypoxic conditions and their activity leads to pH imbalance in tumor tissues and thus provides favorable environment for the survival of cancer cells [13, 14]. Moreover, it contributes to cancer progression by stimulating cancer cell migration, adhesion and invasion. Now a day's CAIX has been identified as an important biomarker of hypoxia and its over-expression is often associated with a poor responsiveness to the classical radio and chemotherapies [15, 16]. Therapeutic inhibition of CAIX has been shown to decrease primary tumor growth and metastasis in various tumor models [17].

Inorganic anions, sulfonamides, sulfamates, sulfamides, phenols are important class of pharmacophores that inhibit CAIX very efficiently by participating in Zn binding [18-20]. Acetazolamide **1** (**Figure S1**) is a potent CA inhibitor which inhibits CA isoform in a nonselective manner through participating in Zn-binding [21]. Recently, Korkmaz et al. [22] reported a series of phenyl thiourea derivatives as novel class of CA inhibitors. In this series derivative **2 (Figure S1)** inhibit CA with micro molar range activities. Coumarins appeared as new class of CAIs that binds (in hydrolyzed form) at the entrance of the CA active site and does not interact with the Zn metal. Thiocoumarine derivatives **3** (**Figure S1**) exhibits an excellent inhibitory activity for CAIX without showing Zn metal binding in active site of CA [23]. Moreover, coumarin derivative **4** (**Figure S1**) was also successfully inhibits CA isoform without displaying Zn-binding [24]. Thus, coumarins show entirely new category of mechanism to inhibit CA enzyme. Numerous, potent sulfonamide based CAIX inhibitors have already been identified in the last years that can efficiently inhibit CAIX activity [22]. However, most of the clinically used CA-inhibitors exhibit broad CA-inhibition and possesses poor isozyme subtype selectivity [25, 26]. Therefore, a selective CAIX inhibitor is essentially required in cancer therapy without side effects related to the inhibition of other CA isozymes [2, 27]. Novel chemical scaffolds which endowed with improved activity as well as selectivity for CAIX are essentially required for the development of successful anticancer agents.

Triazoles have emerged as an important class of heterocyclic compound to design potent therapeutic drug molecules [28]. Numerous triazole derivatives have already showed promising anticancer activity in various *in vitro* as well as *in vivo* models [29-31]. Recently, triazole-linked O-glycosides (compound **5**, **Figure S1**) have been used as a selective and potent CAIX inhibitor [27]. Moreover, pyrimidine derivatives (compound **6**, **Figure S1**) also displayed potent CA

inhibitory activity. [32, 33]. Hence, triazole coupled pyrimidine molecules would be a promising scaffold for the development of potent and selective CAIX inhibitors towards the cancer therapy.

In this view, we have design and synthesized urea pendant triazolo-pyrimidine derivatives (TPUI and TPUII) as a novel class of CAIX inhibitors **(Figure S1, compound 7).** The designed molecules are endowed with essential pharmacophoric requirement such as hydrophobic domain (triazolo-pyrimidine) as well as hydrogen bond donor (HBD)/ hydrogen bond acceptor (HBA) (Urea fragment) domain (**Figure S1**). The designed compounds have a urea functional group instead of the traditional sulfonamide group. This alteration might open a new door for a novel class of pharmacophore as selective CAIX inhibitors. Binding affinities of TPUI and TPUII with CAIX as well as CAII were assessed by spectrofluorimeter. *In vitro* CA inhibition studies of TPUI and TPUII against CAIX as well as CAII were studied by the 4-NPA spectrophotometric assay. Moreover, CAIX selective derivative TPUI was docked with human CAIX to evaluate its interaction potential and sitting pattern in active site CAIX isoforms. Furthermore, MD simulation studies were also performed to evaluate the extensive binding prototype of synthesized triazolo-pyrimidine urea derivatives with CAIX.

2. Materials and Methods

2.1. Synthesis of TPUI and TPUII

All chemicals, reagents and solvents were procured from Sigma Aldrich (St. Louis, MO, USA), S.D Fine Chemicals (India) and Merck (Darmstadt, Germany). The homogeneity and purity of the compounds were checked by thin layer chromatography (TLC), performed on commercially available silica gel (Kieselgel 60, F_{254}) coated aluminium sheets (Merck) by using methanol:

chloroform (5:95) as solvent system. The visualization on TLC was done by both ultra-violet (UV) light (λ= 254 nm) and iodine indicator. All compounds were purified by column chromatography by using silica gel 100-200 mesh (Merck). Melting points were determined in open capillary tubes in a Hicon melting point apparatus (Hicon, India). The nuclear magnetic resonance (NMR) spectra were obtained on high resolution Jeol-400MHz NMR spectrophotometer (USA) in $CDCl_3$ and DMSO-d_6 using Tetramethylsilane (TMS) as the internal reference. Chemical shifts (δ) were expressed in parts per million relative to TMS and the following abbreviations were used to describe the peak patterns when appropriate: s, (singlet); d, (doublet); t, (triplet); m, (multiplet); brs, (broad singlet); dd, (double doublet).The coupling constant (*J*) values are given in hertz (Hz). Mass spectra (LRMS) were recorded on an Agilent 6310 Ion trap LC/MS and elemental analysis (C, H and N) was carried on Elementar analysensysteme. A detail of chemical analysis is provided in the Supplementary Text for Chemistry Section.

2.2. Cloning, Expression and Purification of CAIX and CAII

The 1131-bp coding region (38-414aa) of catalytic domain of CAIX gene was sub-cloned into pET21c (Novagen) vector with the C-terminal His6 tag. Similarly, CAII gene of 801-bp was sub-cloned into pET15d vector (Novagen) with N-terminal His6Xtag. Both proteins were expressed in *Escherichia* coli BL21 (DE3) cells. CAIX was expressed at 16 °C for 14 hours after induction with 0.5mM IPTG (Sigma). CAIX was expressed as insoluble protein and form inclusion bodies (IBs) and pellets were dissolved in the suspension buffer (50 mM phosphate, pH 7.4, 300 mM NaCl, 1% Triton-X and 1% N-lauroylsarcosine) to solubilize IBs. These solubilized IBs were sonicated and centrifuged for 30 minutes at 12,000 rpm. This step was repeated thrice and finally supernatant was applied on a Ni-NTA Sepharose column (GE Health-care). CAIX was eluted from the column

with elution buffer (50 mM phosphate, pH 7.4, 300 mM NaCl, 1% N-lauroylsarcosine and 350 mM imidazole). CAIX was refolded by dialyzing against refolding buffer (50 mM phosphate buffer pH 7.4 and 150 mM NaCl) for 36 hrs at 4ºC with five successive buffer changes. We also performed enzyme assay of refolded CAIX (*34*). **Figure S2 A and B** are showing the SDS-PAGE and Western blot, respectively of purified CAIX.

CAII was expressed at 37 °C for 3 hours after induction with 0.25 mM IPTG (Sigma) as soluble protein, harvested cells were suspended in buffer (50 mM phosphate, pH 7.4, 300 mM NaCl, 1% Triton-X and 0.1mg/ml lysozyme). Cell lysate was sonicated and centrifuged to remove cell debris. Supernatant was applied to Ni-NTA Sepharose column (GE Health-care) and eluted with elution buffer (50 mM phosphate, pH 7.4, 300 mM NaCl, and 300 mM imidazole). The eluent was collected, concentrated and loaded to gel-filtration chromatography (superdex200, GE Healthcare Bio-Sciences) in 50 mM phosphate, pH 7.4 and 150 mM NaCl buffer (*35*). Both proteins were analyzed by SDS-PAGE and identified by Western blotting with anti-histidine antibodies. **Figure S2 C and D** are showing the SDS-PAGE and Western blot, respectively of purified CAII.

2.3. Fluorescence spectra measurements

Fluorescence measurement was performed in the Jasco spectrofluorimeter (Model FP-6200) using 5 mm quartz cuvette. Protein concentration of 3.4 μM and 2.8 μM were used for CAII and CAIX, respectively. Compounds (TPUI and TPUII) were used in a concentration 1-10 μM. The protein solution was excited at 292 nm, and emission spectra were recorded between 300 - 400 nm. Both compounds were dissolved in DMSO and then diluted to 1 mg/ml in the 50 mM phosphate buffer pH 7.4 and 150 mM NaCl. The protein solution was titrated with increasing concentration of ligands and a final spectrum was collected after subtracting intensity of the buffer/ligand from each

spectrum. The decrease in fluorescence intensity is due to the addition of ligand has been used to calculate the binding affinity by Stern-Volmer equations with slight modification [34].

$$\log(Fo-F)/F = \log K_a + n\log[Q] \quad (1)$$

Where, F_o is the fluorescence intensity of protein and F is the fluorescence intensity of ligand, K_a is the binding constant and n is the number of binding sites, Q represents quenching constant. For the ligand-protein complex, the values for K_a and n can be derived from the intercept and slope.

2.4. Carbonic anhydrase inhibition assay

Carbonic anhydrase inhibition was measured by previously reported method [35] based on the principle that p-nitrophenol acetate (4-NPA) is hydrolyzed by CA to form p-nitophenol which was measured in Jasco UV/visible spectrophotometer (Jasco V-660, Model B 028661152) equipped with peltier-type temperature controller (ETCS). Absorption was measured at 415 nm using 1 cm path length cuvettes. Reaction mixture contained 50 mM Tris buffer (pH 7.5), 3 mM substrate p-nitrophenol acetate, different concentration of test compounds (0.5 mM) and protein concentration was used 5 µM - 10 µM. All experiments were carried out at least three times at 25 ±.1 ^{o}C. After 3 min incubation at 25 ^{o}C reading was measured.

2.5. Molecular docking

Atomic coordinates of CAIX and CAII were taken from the Protein Data Bank (www.rcsb.org) [36, 37]. Steepest descent method from Gromacs 4.5.5 was used to optimize the coordinates and both proteins were saved in saved in .pdbqt format to carry docking analysis. AutoDock 4.2 with standard protocol was used to dock the TPUI and TPUII with both isozymes. The Lamarckian

genetic algorithm (LGA) was applied to deal with protein-ligands interactions [38]. The most favourable free binding energy and docking orientations lying within the range of 2.0 Å in root-mean square deviation (rmsd) tolerance were used to cluster the molecule and ranked accordingly. PyMOL was used to visualize molecular interactions. All calculations were carried out on workstation machines running Linux x 86 as operating systems.

2.6. Molecular dynamics simulation

MD simulations were performed with Gromacs 4.5.5 suite of programs, using CHARMm force-field and spc216 water molecules. The trajectory files were analysed using GROMACS utilities: g_gyrate, g_rmsd and g_rmsf to obtain the radius of gyration (R*g*), RMSD and root mean square fluctuation (RMSF). The coordinates of CAIX (PDB ID: 3IAI) was energy minimized with steepest descent up to a tolerance of 100 kj mol^{-1} to remove bad contacts. Two independent MD simulations were carried out with standard protocol in water for CAIX and CAIX-TPUI complex at 300K, respectively to evaluate the structural changes, binding affinity and stability in course of simulation. SwissParam server is used to generate the topology file for ligand [39]. The SHAKE algorithm was used to restrain the covalent bonds containing hydrogen atoms at their equilibrium distances and periodic boundary conditions were applied. Particle Mesh Ewald (PME) method was used for computing the long-range electrostatic interactions. A 1.4 nm cut-off for van der Waal interactions and a 1.0 nm cut-off for Coulombs interaction were adopted in the simulation, respectively. Analytical graphs were plotted using Xmgrace, VMD and PyMol were used for structure and molecular interaction analysis [40].

3. Results and discussion

3.1. Chemistry

Synthesis of TPUI and TPUII has been performed according to scheme 1 [41, 42] **(Supplementary Text).** Briefly, aniline/p-fluoroaniline was converted into respective azides by treating sodium nitrate as well as sodium azide in HCl at RT. Equimolar ratio of azides 3-4 and cyanoacetamide has been refluxed in ethanol to get amide derivatives 5 and 6. Further, dehydration of amide derivatives has been done with $POCl_3$ in acetonitrile to achieved cyanotriazole derivatives 7 and 8. Extension of amino functional group of triazole 7 and 8 has been completed with refluxing triethyl orthoformate in acetic anhydride. Cyclized triazolo-pyrimidine urea derivatives 11(TPUI) and 12 (TPUII) were synthesized by reacting semicarbazide with Schiff base intermediate 9 and 10 in ethanol by using triethylamine as basic catalyst. Synthesized compounds were successfully characterized by NMR, mass spectrometry and elemental analysis.

3.2. Florescence binding study

The fluorescence emission spectra of CAIX solution in the absence and presence of different concentrations of compounds (TPU-I and TPU-II) in PBS at 25°C are shown in **Fig. 1A and 1C.** The maximum emission peak was observed at 343 nm (excitation wavelength was 292 nm). Upon incubation of different concentrations (1-10 μM) of compounds with CAIX the maximum fluorescence peak intensity was reduced significantly indicating that CAIX-compound complexes were formed. Change in the intrinsic fluorescence intensity of CAIX was observed when compounds bind to CAIX. The values fluorescence intensity at 343 nm was plotted as a function of [ligand] to calculate the binding affinity (**Figure 1B and 1D.)**.

A similar fluorescence quenching results were observed for CAII with same compounds but their binding affinities are comparatively low (**Figure 2)**. The binding affinity of TPUI for CAII and CAIX are 111.223 μM and 0.048641 μM **(Fig. 1B and 2B).** TPUII showed binding affinity for CAII and CAIX are 240.98 μM and 7.52 μM **(Fig. 1D and 2D).** Results clearly indicate that TPUI exhibited greater affinity for CAIX over CAII as compared to TPUII. It is analyzed that introduction of fluorine atom at para-position on phenyl ring of triazolopyrimidine loss affinity for CAIX as compared to phenyl ring containing triazolopyrimidine.

3.3. Carbonic anhydrase inhibition

Inhibition activities of TPUI, TPUII and AZM were measured against CAII and CAIX by previously reported 4-NPA assay [35]. Inhibition studies results showed that the TPUI possessed 16% and 53% inhibition activities against CAII and CAIX, respectively. Moreover, TPUII possessed 43% and 54% inhibition activities against CAII and CAIX, respectively. Standard inhibitor AZM showed 76% inhibition for CAII and 63% inhibition for CAIX. Our study clearly indicates that TPUI is selectively inhibits CAIX (53%) over CAII (16%) as compared to AZM which did not displayed impressive selective inhibition profile for both CAIX (76%) and CAII (63%). These inhibition results are also consistent with florescence binding studies where TPUI showed good affinity towards CAIX as compared to CAII.

3.4. Molecular docking

Docking analysis of TPUI was carried with both isozymes CAII and CAIX to elucidate interaction pattern of synthesized inhibitors. Result showed that TPUI is nicely bounded into the active site of CAIX with minimum binding energy (ΔG) -10.89 kcal/mol (K_i= 0.032 μM) (Table 1). Although,

TPUI does not bind with Zn^{2+} metal in active site but the best binding mode of TPUI in the active site of CAIX is stabilized with four H-bond interaction with His 94, His119, Thr199 and Thr200 **(Figure 3A).** Active site residues Leu98, Val121, Val143, Leu198 and Trp209 are involved in hydrophobic interaction and Trp5 is stabilized phenyl moiety of triazolo-pyrimidine with π-π interaction **(Figure 3B).** Structure of TPU scaffold is provided in the Figure 3C.

Molecular docking result with CAII shows binding affinity -9.47 kcal/mol (K_i= 87.32 μM) for TPUI **(Figure 4A).** At the active site of CAII, TPUI shows H-bond interaction with Tyr7, Asn67, His96, Thr200, Asn244, whereas residues Ala65, Phe66, Trp97, Leu98 and Val121, Val143, Leu198 and Trp209 are involved in hydrophobic interaction **(Figure 4B).** The phenyl moiety of TPUI is stabilized with π-π interaction of Phe95 and Phe131. Active site topology of CAII is highly conserved with CAIX [2, 36]. However, molecular docking result shows a quite different orientation of TPUI at the active site of CAII (Table 2) and anchored near the outer hydrophobic core of active site and is largely stabilized with Ala65, Phe66, Trp97, Leu98 and Val121, Val143, Leu198 and Trp209.

Structural analysis shows that CAIX active site is located in a large conical cavity which spans from the surface to the centre of isozyme and zinc ion (Zn^{2+}) is coordinated with imidazole ring of three histidine molecules (His-64, His-94 and His-119), at the bottom of cavity [36]. And active site cavity is well partitioned in lower and upper hydrophobic domain and core region is rich in hydrophilic amino acid residues [27, 36]. Whereas, CAII active site is comprised with two distinct domain (i) upper layer is lined with hydrophobic residues: Ile91, Val121, Phe131, Val135, Leu141, Val143, Leu198, Pro202, Leu204, Val207 and Trp 209 (ii) lower domain is facilitated with hydrophilic residues Tyr7, Asn62, His64, Asn67, Thr199 and Thr200 [43] **(Figure 3 and 4).** This

analysis shows that hydrophilic core residues CAII are highly conserved with CAIX. However, the residual difference at the outer linings of CAII active site, specially the hydrophobic residues, facilitated the binding of TPUI towards the outer surface of CAII. Moreover, the compressed outer rim of CAII active site, probably hitched the binding of triazolopyrimidine urea and major interaction is observed at surface. The surface view of both isozymes docked with TPUI is shown in **(Figure 5A and 5B).**

Result shows that interaction and environment at the binding site of CAIX is more favourable for TPUI. Moreover, docking result clearly indicates that TPUI binds in CAIX and CAII with totally different manner (Table 1). TPUI participates in hydrogen bonding interaction with His94, His119, Thr199 and Thr200 in active site of CAIX and exhibits hydrogen bonding interaction with Tyr7, Asn67, His96, Thr200, Asn244 in active site of CAII **(Figure 3, 4 and Table 1).** Moreover, orientation of TPUI in CAIX and CAII was absorbed totally different. Additionally, docking studies show that TPU has emerged as novel class of selective CAIX inhibitor which did not interact with Zn^{+} metal but exhibited excellent binding pattern in active site of CAIX.

3.5. MD simulations

Docking procedures are used to predict the affinity between the ligand and protein through the identification of correct conformation of ligands in the binding pocket of any protein [44-48]. However, MD simulation provides a dynamic picture of protein ligand interactions [49-55]. In the present study, best binding conformation of TPUI into the binding site of CAIX, having highest docking score was taken for further analysis. We performed 40 ns MD simulation and found that TPUI remain inside the binding pocket of CAIX. Dynamic stability of CAIX and its complex with TPUI, over the simulation of 40 ns was analyzed using backbone RMSD of C^{α} atoms. RMSD

result shows a stable conformation is maintained throughout the simulation time of 40 ns. Plot of time versus RMSD is shown in **Figure 6A.**

Trajectory for CAIX achieved a stable equilibrium in 5 ns, with the initial drift of 0.05 nm. A small transition in trajectory is observed after 20 ns which is repeated up to 30 ns with drift of 0.05 nm. However, trajectory attains the stability after 30 ns and a continuous equilibrium is maintained up to end of simulation time. RMSD plot of CAIX-TPUI complex shows a significant drift of ~ 0.1 nm at 15 ns, indicates the conformational change in CAIX, due to spatial fitting of TPUI in the active site. The small but continuous rise in trajectory represented the various interactions with ligand. The trajectory for isozyme became stable after 25 ns with drop down of 0.08 nm and further, it maintained stable conformation throughout the simulation time of 40 ns. The less change in RMSD of backbone atoms strongly suggests the stable dynamic behaviour of CAIX-TPUI complex.

Furthermore, the *R*g analysis is carried to measure the compactness of isozyme. The average value of Rg, calculated from trajectory is shown in **Figure 6B.** Plot for CAIX, clearly indicates that a steady *R*g value 1.77 nm is maintained over the course of 40 ns. The average Rg value of 1.70 nm is found for CAIX-TPUI complex showed the stable isozyme-inhibitor interaction. The relative decrease in *R*g (0.07 nm), lead to increase in compactness of isozyme, suggests that binding of TPUI may enhance the stability of isozyme. The stable back bone RMSD and decrease in *R*g score from native structure strongly indicate that association of TPUI with CAIX is retained during the entire simulation time.

The average position fluctuation of residues in a dynamic system is analysed with RMSF of all C^{α} atoms. **Figure 6C** clearly shows residues belong to stable secondary structure conformation (α/β

sheet) have stable fluctuation. The residues having higher fluctuations are belonging to loops. Result shows binding of TPUI lead to increase fluctuation of active site residues. This observation is consistent with RMSD and *R*g data, and result revelled H-bond interaction with His94, His96, His119, Thr199 and Thr200 plays important role in activity of CA inhibitors. Upper and lower hydrophobic domains are essential to anchor inhibitor at the active site of isozyme. Moreover, amino acid differences in the hydrophobic domain of CAIX and CAII are significantly important for the selective binding TPUI and TPUII with isozyme CAIX. Result showed that hydrophobic domain may be good target for the design of isozyme selective inhibitor. To gain insight into the effect of active site residues involve in interaction with inhibitor, we carried solvent accessible surface area of the CAIX (**Figure 6D**) and result is found to consistent with RMSF. MD simulation is precisely used to evaluate the molecular docking results.

4. Conclusions

The rational drug design for selective inhibition of CA isozymes is a difficult target, due to conservation of active site structure and topology within the CA enzyme family. However, the selective inhibition of CAIX is essentially required for cancer therapy without side effect associated with CAII inhibition. Here we have successfully designed and synthesized TPUI and TPUII as potent and selective CAIX inhibitors. Both TPUI and II appeared as potent CAIX inhibitor *in silico* as well as *in vitro* studies. However, TPUI displayed greater inhibition activity and selectivity for CAIX isozyme. These studies successfully provided an endeavour for the rational design of triazolopyrimidine urea as a novel class of CAIX inhibitor. This molecule may be explored as lead in development of selective CAIX inhibitor for the therapy of various cancers in future.

Conflict of interest

Authors declare no conflict of interest regarding any financial and personal relationships with other people or organizations that could inappropriately influence (bias) this work.

Acknowledgements

SK, DI, AP and CMB are thankful to University Grants Commission (UGC), New Delhi, India, for their fellowship. MT is thankful to University of Delhi for providing financial support. Authors sincerely thank Jamia Millia Islamia for providing high speed server in the Central Instrumentation Facility. Harvard University-plasmid facility is acknowledged providing the *CAVA* gene. FA and MIH are thankful to the Department of Science and Technology (Government of India) and Indian Council for Medical Research (ICMR) for financial support. Authors thank Department of Science and Technology, Government of India for FIST support (SR/FST/LSI-541/2012).

References

1. Alterio V, Di Fiore A, D'Ambrosio K, Supuran CT, De Simone G. Multiple binding modes of inhibitors to carbonic anhydrases: how to design specific drugs targeting 15 different isoforms? *Chem Rev* 2012,**112**:4421-4468.

2. Imtaiyaz Hassan M, Shajee B, Waheed A, Ahmad F, Sly WS. Structure, function and applications of carbonic anhydrase isozymes. *Bioorg Med Chem* 2013,**21**:1570-1582.

3. Reibring CG, El Shahawy M, Hallberg K, Kannius-Janson M, Nilsson J, Parkkila S*, et al.* Expression patterns and subcellular localization of carbonic anhydrases are developmentally regulated during tooth formation. *PLoS One* 2014,**9**:e96007.

4. D'Ambrosio K, Carradori S, Monti SM, Buonanno M, Secci D, Vullo D*, et al.* Out of the active site binding pocket for carbonic anhydrase inhibitors. *Chem Commun (Camb)* 2015,**51**:302-305.

5. Salmon AJ, Williams ML, Wu QK, Morizzi J, Gregg D, Charman SA*, et al.* Metallocene-based inhibitors of cancer-associated carbonic anhydrase enzymes IX and XII. *J Med Chem* 2012,**55**:5506-5517.

6. Doyen J, Parks SK, Marcie S, Pouyssegur J, Chiche J. Knock-down of hypoxia-induced carbonic anhydrases IX and XII radiosensitizes tumor cells by increasing intracellular acidosis. *Front Oncol* 2012,**2**:199.

7. Nocentini A, Carta F, Ceruso M, Bartolucci G, Supuran CT. Click-tailed coumarins with potent and selective inhibitory action against the tumor-associated carbonic anhydrases IX and XII. *Bioorg Med Chem* 2015.

8. Syrjanen L, Luukkaala T, Leppilampi M, Kallioinen M, Pastorekova S, Pastorek J*, et al.* Expression of cancer-related carbonic anhydrases IX and XII in normal skin and skin neoplasms. *APMIS* 2014,**122**:880-889.

9. Hynninen P, Vaskivuo L, Saarnio J, Haapasalo H, Kivela J, Pastorekova S*, et al.* Expression of transmembrane carbonic anhydrases IX and XII in ovarian tumours. *Histopathology* 2006,**49**:594-602.

10. Dudutiene V, Matuliene J, Smirnov A, Timm DD, Zubriene A, Baranauskiene L*, et al.* Discovery and characterization of novel selective inhibitors of carbonic anhydrase IX. *J Med Chem* 2014,**57**:9435-9446.

11. Gluszok S, Frederick R, Foulon C, Klupsch F, Supuran CT, Vullo D*, et al.* Design, solid-phase synthesis, and biological evaluation of novel 1,5-diarylpyrrole-3-carboxamides as carbonic anhydrase IX inhibitors. *Bioorg Med Chem* 2010,**18**:7392-7401.

12. Morris JC, Chiche J, Grellier C, Lopez M, Bornaghi LF, Maresca A, *et al.* Targeting hypoxic tumor cell viability with carbohydrate-based carbonic anhydrase IX and XII inhibitors. *J Med Chem* 2011,**54**:6905-6918.

13. Supuran CT. Development of small molecule carbonic anhydrase IX inhibitors. *BJU Int* 2008,**101 Suppl 4**:39-40.

14. Idrees D, Prakash A, Haque MA, Islam A, Ahmad F, Hassan MI. Spectroscopic and MD simulation studies on unfolding processes of mitochondrial carbonic anhydrase VA induced by urea. *J Biomol Struct Dyn* 2015:1-37.

15. Vullo D, Franchi M, Gallori E, Pastorek J, Scozzafava A, Pastorekova S, *et al.* Carbonic anhydrase inhibitors: inhibition of the tumor-associated isozyme IX with aromatic and heterocyclic sulfonamides. *Bioorg Med Chem Lett* 2003,**13**:1005-1009.

16. Wang L, Yang C, Lu W, Liu L, Gao R, Liao S, *et al.* Discovery of new potent inhibitors for carbonic anhydrase IX by structure-based virtual screening. *Bioorg Med Chem Lett* 2013,**23**:3496-3499.

17. Thobani A, Fishman GA. The use of carbonic anhydrase inhibitors in the retreatment of cystic macular lesions in retinitis pigmentosa and X-linked retinoschisis. *Retina* 2011,**31**:312-315.

18. Altintop MD, Ozdemir A, Kucukoglu K, Turan-Zitouni G, Nadaroglu H, Kaplancikli ZA. Synthesis and evaluation of new thiadiazole derivatives as potential inhibitors of human carbonic anhydrase isozymes (hCA-I and hCA-II). *J Enzyme Inhib Med Chem* 2015,**30**:32-37.

19. SitaRam, Ceruso M, Khloya P, Supuran CT, Sharma PK. 4-Functionalized 1,3-diarylpyrazoles bearing 6-aminosulfonylbenzothiazole moiety as potent inhibitors of carbonic anhydrase isoforms hCA I, II, IX and XII. *Bioorg Med Chem* 2014,**22**:6945-6952.

20. SitaRam, Celik G, Khloya P, Vullo D, Supuran CT, Sharma PK. Benzenesulfonamide bearing 1,2,4-triazole scaffolds as potent inhibitors of tumor associated carbonic anhydrase isoforms hCA IX and hCA XII. *Bioorg Med Chem* 2014,**22**:1873-1882.

21. Pichake J, Kharkar PS, Ceruso M, Supuran CT, Toraskar MP. Carbonic anhydrase inhibitors: design, synthesis, and biological evaluation of novel sulfonyl semicarbazide derivatives. *ACS Med Chem Lett* 2014,**5**:793-796.

22. Korkmaz N, Obaidi OA, Senturk M, Astley D, Ekinci D, Supuran CT. Synthesis and biological activity of novel thiourea derivatives as carbonic anhydrase inhibitors. *J Enzyme Inhib Med Chem* 2015,**30**:75-80.

23. Maresca A, Temperini C, Pochet L, Masereel B, Scozzafava A, Supuran CT. Deciphering the mechanism of carbonic anhydrase inhibition with coumarins and thiocoumarins. *J Med Chem* 2010,**53**:335-344.

24. Maresca A, Temperini C, Vu H, Pham NB, Poulsen SA, Scozzafava A, *et al.* Non-zinc mediated inhibition of carbonic anhydrases: coumarins are a new class of suicide inhibitors. *J Am Chem Soc* 2009,**131**:3057-3062.

25. Carradori S, De Monte C, D'Ascenzio M, Secci D, Celik G, Ceruso M, *et al.* Salen and tetrahydrosalen derivatives act as effective inhibitors of the tumor-associated carbonic anhydrase XII--a new scaffold for designing isoform-selective inhibitors. *Bioorg Med Chem Lett* 2013,**23**:6759-6763.

26. Cecchi A, Taylor SD, Liu Y, Hill B, Vullo D, Scozzafava A, *et al.* Carbonic anhydrase inhibitors: inhibition of the human isozymes I, II, VA, and IX with a library of substituted difluoromethanesulfonamides. *Bioorg Med Chem Lett* 2005,**15**:5192-5196.

27. Prakash A, Kumar K, Islam A, Hassan MI, Ahmad F. Receptor Chemoprint Derived Pharmacophore Model for Development of CAIX Inhibitors. *J Carcinog Mutagen* 2013,**S8**:1-9.

28. Wilkinson BL, Bornaghi LF, Houston TA, Innocenti A, Supuran CT, Poulsen SA. A novel class of carbonic anhydrase inhibitors: glycoconjugate benzene sulfonamides prepared by "click-tailing". *J Med Chem* 2006,**49**:6539-6548.

29. Akula NV, Kumar S, Singh V, Tiwari M. Homology modeling and QSAR analysis of 1,3,4-thiadiazole and 1,3,4-triazole derivatives as carbonic anhydrase inhibitors. *Indian J Biochem Biophys* 2010,**47**:234-242.

30. Almajan GL, Barbuceanu SF, Innocenti A, Scozzafava A, Supuran CT. Carbonic anhydrase inhibitors. Inhibition of the cytosolic and tumor-associated carbonic anhydrase isozymes I, II and IX with some 1,3,4-oxadiazole- and 1,2,4-triazole-thiols. *J Enzyme Inhib Med Chem* 2008,**23**:101-107.

31. Grandane A, Tanc M, Zalubovskis R, Supuran CT. Synthesis of 6-tetrazolyl-substituted sulfocoumarins acting as highly potent and selective inhibitors of the tumor-associated carbonic anhydrase isoforms IX and XII. *Bioorg Med Chem* 2014,**22**:1522-1528.

32. Riafrecha LE, Rodriguez OM, Vullo D, Supuran CT, Colinas PA. Attachment of carbohydrates to methoxyaryl moieties leads to highly selective inhibitors of the cancer associated carbonic anhydrase isoforms IX and XII. *Bioorg Med Chem* 2014,**22**:5308-5314.

33. Wilkinson BL, Bornaghi LF, Houston TA, Innocenti A, Vullo D, Supuran CT, *et al.* Carbonic anhydrase inhibitors: inhibition of isozymes I, II, and IX with triazole-linked O-glycosides of benzene sulfonamides. *J Med Chem* 2007,**50**:1651-1657.

34. Wang YQ, Zhang HM, Zhang GC, Tao WH, Fei ZH, Liu ZT. Spectroscopic studies on the interaction between silicotungstic acid and bovine serum albumin. *J Pharm Biomed Anal* 2007,**43**:1869-1875.

35. Pocker Y, Stone JT. The catalytic versatility of erythrocyte carbonic anhydrase. 3. Kinetic studies of the enzyme-catalyzed hydrolysis of p-nitrophenyl acetate. *Biochemistry* 1967,**6**:668-678.

36. Alterio V, Hilvo M, Di Fiore A, Supuran CT, Pan P, Parkkila S, *et al.* Crystal structure of the catalytic domain of the tumor-associated human carbonic anhydrase IX. *Proc Natl Acad Sci U S A* 2009,**106**:16233-16238.

37. Vidgren J, Liljas A, Walker NP. Refined structure of the acetazolamide complex of human carbonic anhydrase II at 1.9 A. *Int J Biol Macromol* 1990,**12**:342-344.

38. Fuhrmann J, Rurainski A, Lenhof HP, Neumann D. A new Lamarckian genetic algorithm for flexible ligand-receptor docking. *J Comput Chem* 2010,**31**:1911-1918.

39. Zoete V, Cuendet MA, Grosdidier A, Michielin O. SwissParam: a fast force field generation tool for small organic molecules. *J Comput Chem* 2011,**32**:2359-2368.

40. Lill MA, Danielson ML. Computer-aided drug design platform using PyMOL. *J Comput Aided Mol Des* 2011,**25**:13-19.

41. Chen X, Shi D. Synthesis and biological activity of 3-[(6-chloropyridin-3-yl)methyl]-6-substituted-6,7-dihydro-3H-1,2,3-triazolo[4,5-d]-pyrimidin-7-imines *J Heterocylic Chem* 2008,**45**:1493-1497.

42. Ried W, Laoutidis J. Synthese neuartiger triazoloanellierter 8-Azapurine *Liebigs Annalen der Chemie* 1988,**11**:1107-1109.

43. Tanpure RP, Ren B, Peat TS, Bornaghi LF, Vullo D, Supuran CT, *et al.* Carbonic anhydrase inhibitors with dual-tail moieties to match the hydrophobic and hydrophilic halves of the carbonic anhydrase active site. *J Med Chem* 2015,**58**:1494-1501.

44. Thakur PK, Kumar J, Ray D, Anjum F, Hassan MI. Search of potential inhibitor against New Delhi metallo-beta-lactamase 1 from a series of antibacterial natural compounds. *J Nat Sci Biol Med* 2013,**4**:51-56.

45. Naz F, Shahbaaz M, Bisetty K, Islam A, Ahmad F, Hassan MI. Designing New Kinase Inhibitor Derivatives as Therapeutics Against Common Complex Diseases: Structural Basis of Microtubule Affinity-Regulating Kinase 4 (MARK4) Inhibition. *OMICS* 2015,**19**:700-711.

46. Naz F, Shahbaaz M, Khan S, Bisetty K, Islam A, Ahmad F, *et al.* PKR-inhibitor binds efficiently with human microtubule affinity-regulating kinase 4. *J Mol Graph Model* 2015,**62**:245-252.

47. Naz H, Jameel E, Hoda N, Shandilya A, Khan P, Islam A, *et al.* Structure guided design of potential inhibitors of human calcium-calmodulin dependent protein kinase IV containing pyrimidine scaffold. *Bioorganic & Medicinal Chemistry Letters* 2016:(In Press).

48. Aneja B, Irfan M, Hassan MI, Prakash A, Yadava U, Daniliuc CG*, et al.* Monocyclic beta-lactam and unexpected oxazinone formation: synthesis, crystal structure, docking studies and antibacterial evaluation. *J Enzyme Inhib Med Chem* 2015:1-19.

49. Hoda N, Naz H, Jameel E, Shandilya A, Dey S, Hassan MI*, et al.* Curcumin specifically binds to the human calcium-calmodulin-dependent protein kinase IV: fluorescence and molecular dynamics simulation studies. *J Biomol Struct Dyn* 2015:1-13.

50. Anwer K, Sonani R, Madamwar D, Singh P, Khan F, Bisetty K*, et al.* Role of N-terminal residues on folding and stability of C-phycoerythrin: simulation and urea-induced denaturation studies. *J Biomol Struct Dyn* 2015,**33**:121-133.

51. Devika NT, Amresh P, Hassan MI, Ali BM. Molecular modeling and simulation of the human eNOS reductase domain, an enzyme involved in the release of vascular nitric oxide. *J Mol Model* 2014,**20**:2470.

52. Haque MA, Zaidi S, Ubaid-Ullah S, Prakash A, Hassan MI, Islam A*, et al.* In vitro and in silico studies of urea-induced denaturation of yeast iso-1-cytochrome c and its deletants at pH 6.0 and 25 degrees C. *J Biomol Struct Dyn* 2015,**33**:1493-1502.

53. Hassan MI, Kumar V, Somvanshi RK, Dey S, Singh TP, Yadav S. Structure-guided design of peptidic ligand for human prostate specific antigen. *J Pept Sci* 2007,**13**:849-855.

54. Khan FI, Shahbaaz M, Bisetty K, Waheed A, Sly WS, Ahmad F*, et al.* Large scale analysis of the mutational landscape in beta-glucuronidase: A major player of mucopolysaccharidosis type VII. *Gene* 2015.

55. Khan P, Parkash A, Islam A, Ahmad F, Hassan MI. Molecular basis of the structural stability of hemochromatosis factor E: A combined molecular dynamic simulation and GdmCl-induced denaturation study. *Biopolymers* 2015.

Figure-1: Fluorescence emission spectra of **(A)** CAIX with TPUI, **(B)** Plot of log (Fo-F)/F vs log [Q] for quenching of CAIX by TPU 1, **(C)** CAIX with TPUII, **(D)** Plot of log (Fo-F)/F vs log [Q] for quenching of CAIX by TPUII.

Figure-2: Fluorescence emission spectra of **(A)** CAII with TPUI, **(B)** Plot of log (Fo-F)/F vs log [Q] for quenching of CAII by TPU 1, **(C)** CAII with TPUII, **(D)** Plot of log (Fo-F)/F vs log [Q] for quenching of CAII by TPUII.

Figure-3: (A) Cartoon view of TPUI docked with CAIX. **(B)** Active site residue interactions with TPUI. Residues are shown with stick and TPUI is shown with ball and stick model. Hydrogen bonds are shown as broken lines (black). **(C).** Chemical structure of TPU scaffold.

Figure-4: (A) Cartoon view of TPUI docked with CAII. **(B)** Active site residues interaction with TPUI. Residues are shown with stick and TPUI is shown with ball and stick model. Hydrogen bonds are shown as broken lines (black).

Figure-5: Surface representation of CAII **(A)** and CAIX, **(B)** docked with TPUI. Hydrophobic core of active site is colored with element.

Figure-6: (A) Plot of time versus RMSD trajectory of isozyme CAIX (blue) and CAIX-TPUI complex (red). **(B)** Time evolution of radius of gyration (*R*g) values during 40,000 ps (40 ns) of MD simulation. The *R*g plot for isozyme CAIX is shown with color black and CAIX-TPUI complex is shown with color red. **(C).** RMSF plot for isozyme CAIX (blue) and CAIX-TPUI complex (red). **(D)** Accessible surfaces area (ASA) plot for isozyme CAIX (blue) and CAIX-TPUI complex (red).

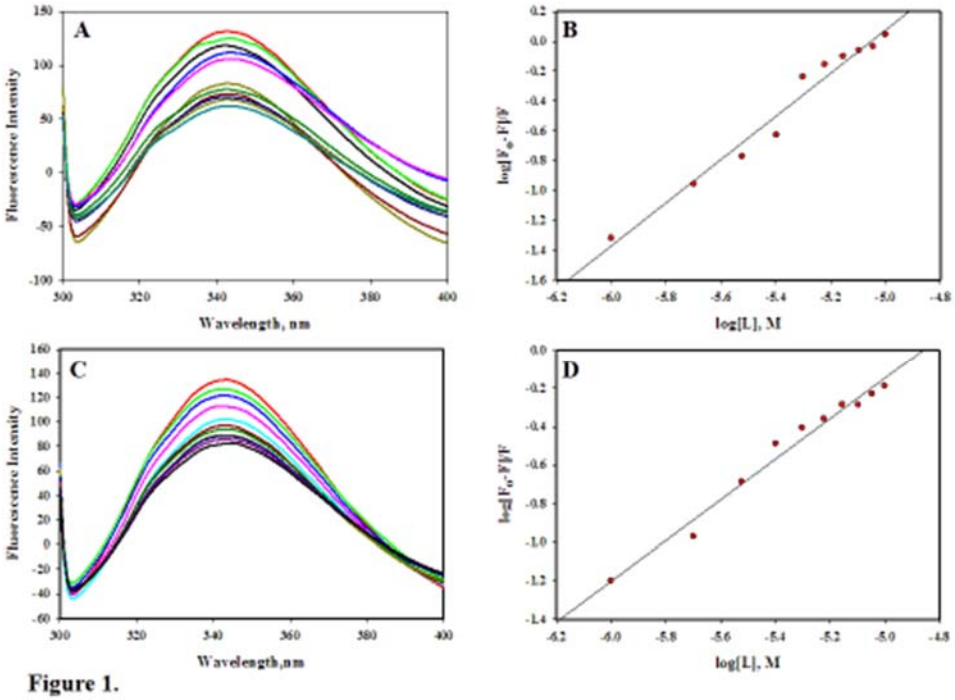

Figure 1.

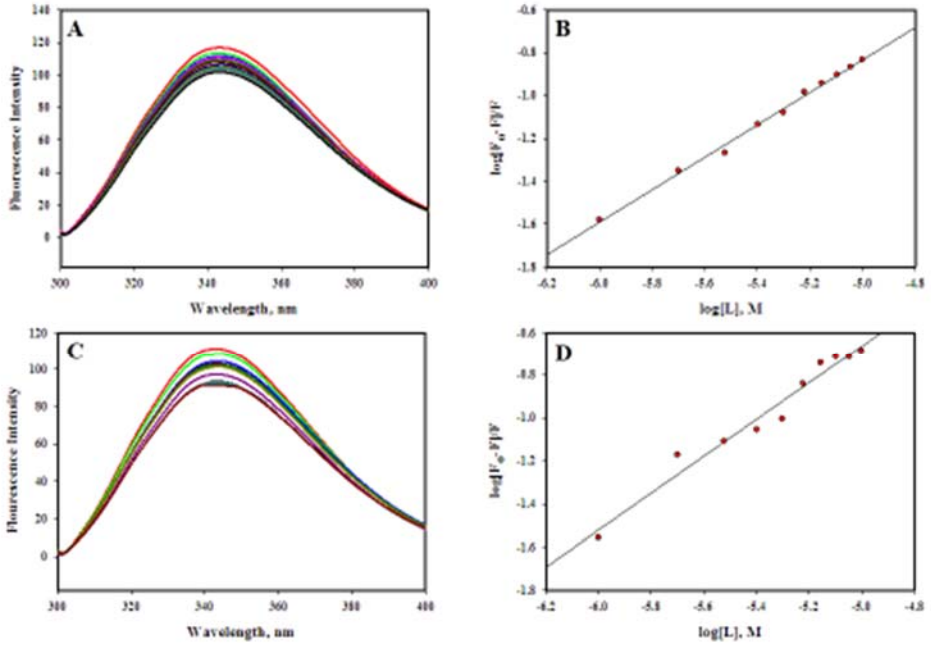

Figure 2.

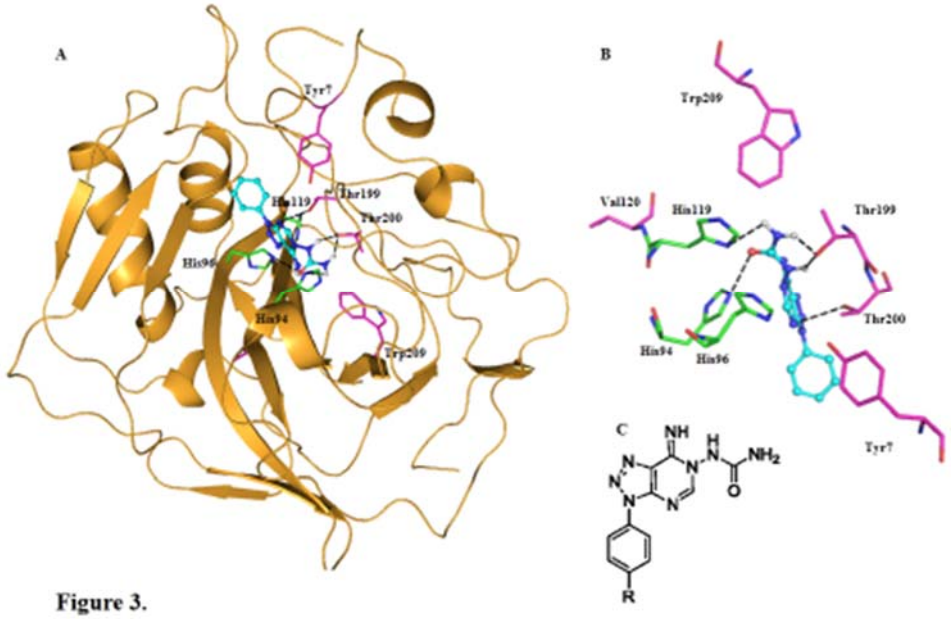

Figure 3.

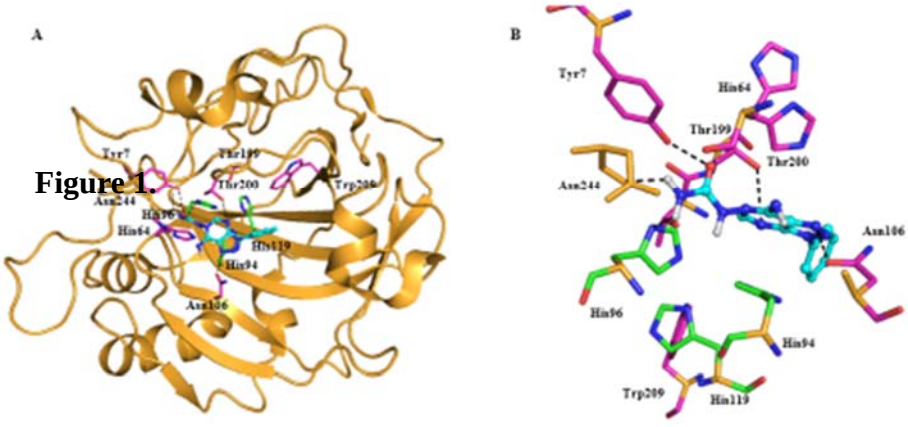

Figure 4.

Figure 1.

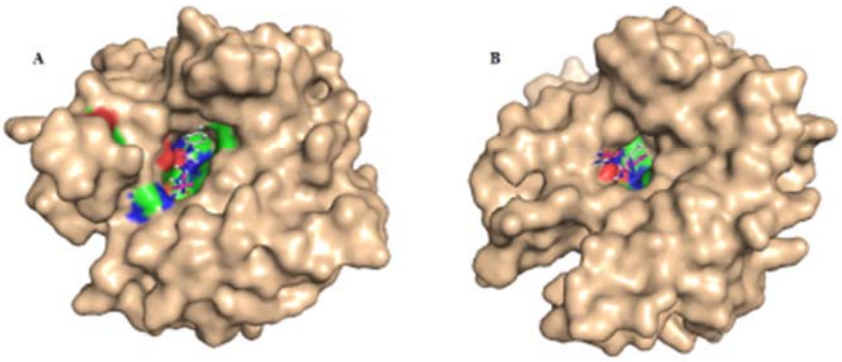

Figure 5.

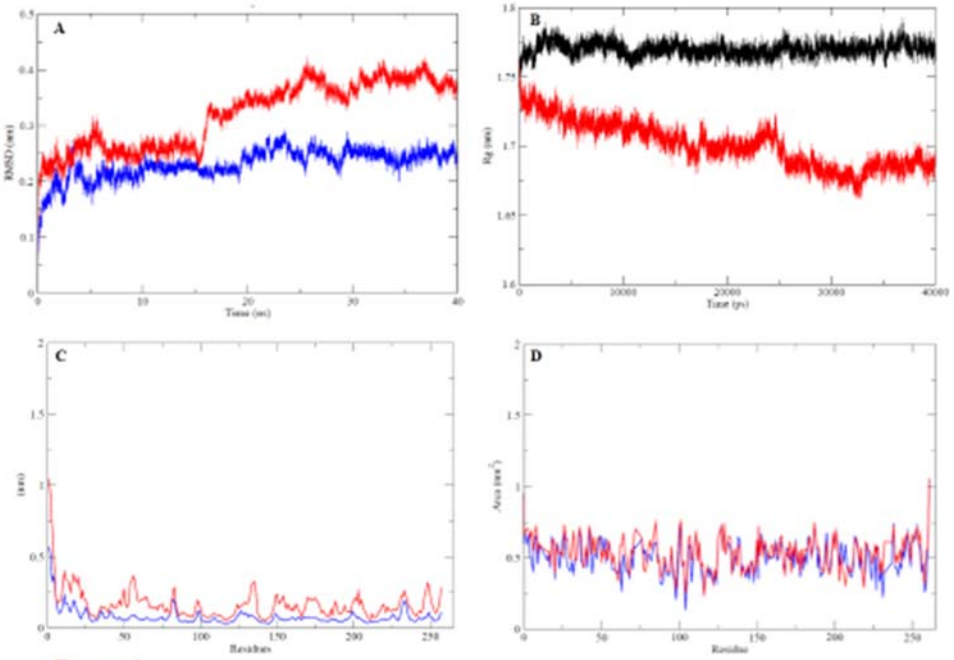

Figure 6.

Table 1: Docking score of TPUI and TPUII

	CA IX		CA IX	
	Binding affinity (ΔG)	Estimated K_i	Binding affinity (ΔG)	Estimated K_i
TPU I	-10.89 kcal/mol	0.032 μM	-9.47 kcal/mol	87.32 μM
TPU II	-10.26 kcal/mol	1.67 μM	-8.53 kcal/mol	192.6 μM

Table 2: Molecular docking binding scores and binding interactions of compounds **TPUI** within the CAIX and CAII active site (<5Å).

Residual interaction of PTU I with CAIX		Residual interaction of PTU I with CAII	
H-bonds	Hydrophobic	H-bonds	Hydrophobic
His 94, His119, Thr199, Thr200	**Trp5,** Leu98, Val121, Val143, Leu198, Trp209	**Tyr7,Asn67,His96**, Thr200, **Asn244**	**Ala65, Phe66, Trp97,** Leu98, Val121, Val143, **Leu204,Val207**, Trp209
Docking score (ΔG) : -10.89 kcal/mol		Docking score (ΔG) : -9.47 kcal/mol	